Proc. Natl. Acad. Sci. USA
Vol. 96, pp. 4273–4278, April 1999
Biochemistry

Structure-based design of submicromolar, biologically active inhibitors of trypanosomatid glyceraldehyde-3-phosphate dehydrogenase

ALEX M. ARONOV*†, STEPHEN SURESH‡§, FREDERICK S. BUCKNER¶, WESLEY C. VAN VOORHIS¶, CHRISTOPHE L. M. J. VERLINDE‡, FRED R. OPPERDOES‖, WIM G. J. HOL*‡**,††, AND MICHAEL H. GELB*,††,‡‡,§§

Departments of *Chemistry, ‡Biological Structure, ¶Medicine, §§Biochemistry, and §Howard Hughes Medical Institute and Biomolecular Structure Center, University of Washington, Seattle, WA 98195; and ‖Research Unit for Tropical Diseases, International Institute of Cellular and Molecular Pathology, Brussels, Belgium

Edited by Stephen J. Benkovic, Pennsylvania State University, University Park, PA, and approved January 6, 1999 (received for review November 3, 1998)

ABSTRACT **The bloodstream stage of *Trypanosoma brucei* and probably the intracellular (amastigote) stage of *Trypanosoma cruzi* derive all of their energy from glycolysis. Inhibiting glycolytic enzymes may be a novel approach for the development of antitrypanosomatid drugs provided that sufficient parasite versus host selectivity can be obtained. Guided by the crystal structures of human, *T. brucei*, and *Leishmania mexicana* glyceraldehyde-3-phosphate dehydrogenase, we designed adenosine analogs as tight binding inhibitors that occupy the pocket on the enzyme that accommodates the adenosyl moiety of the NAD^+ cosubstrate. Although adenosine is a very poor inhibitor, $IC_{50} \approx$ 50 mM, addition of substituents to the 2′ position of ribose and the N^6-position of adenosine led to disubstituted nucleosides with micromolar to submicromolar potency in glyceraldehyde-3-phosphate dehydrogenase assays, an improvement of 5 orders of magnitude over the lead. The designed compounds do not inhibit the human glycolytic enzyme when tested up to their solubility limit (≈40 μM). When tested against cultured bloodstream *T. brucei* and intracellular *T. cruzi*, N^6-(1-naphthalenemethyl)-2′-(3-chlorobenzamido)adenosine inhibited growth in the low micromolar range. Within minutes after adding this compound to bloodstream *T. brucei*, production of glucose-derived pyruvate ceased, parasite motility was lost, and a mixture of grossly deformed and lysed parasites was observed. These studies underscore the feasibility of using structure-based drug design to transform a mediocre lead compound into a potent enzyme inhibitor. They also suggest that energy production can be blocked in trypanosomatids with a tight binding competitive inhibitor of an enzyme in the glycolytic pathway.**

There is tremendous need for new drugs against trypanosomes and leishmania (trypanosomatids). The World Health Organization estimates that 16–18 million people in Latin America are chronically infected with *Trypanosoma cruz*i, the causative agent of Chagas' disease (ref. 1; http://www.who.org). More than 20 million people are infected with *Leishmania spp.,* including *Leishmania mexicana,* the causative agents of visceral and cutaneous Leishmaniasis. African sleeping sickness, caused by *Trypanosoma brucei*, currently is sweeping through sub-Saharan Africa with prevalence reminiscent of the great epidemic of the 1930s, which killed half a million people (2). The diseases caused by these organisms can be fatal if left untreated, and current drug therapy is unsatisfactory because of severe toxicity, resistance, and in some cases the need for parenteral administration (3).

Extensive studies of energy metabolism in *T. brucei* leave no doubt that the bloodstream stage uses glycolysis as its only source of energy (4). Although the study of energy metabolism in *T. cruzi* growing inside of host cells (amastigote stage) is difficult because of complications from host metabolism, biochemical studies with axenic amastigotes suggest that this form uses glycolysis as its major energy source (5). In bloodstream *T. brucei*, glucose is metabolized to pyruvate, which is excreted, and two molecules of ATP are produced. The single, yet critical, role that mitochondria serve in energy production is providing an oxidase for transferring two electrons from NADH, produced during glycolysis by glyceraldehyde-3-phosphate (GAPDH), to oxygen. Electrons are transferred from the site of glycolysis, an organelle called the glycosome, to mitochondria via a glycerol-3-phosphate/dihydroxyacetone phosphate shuttle. *T. brucei* is killed when cultured with a combination of glycerol and salicylhydroxamic acid, an inhibitor of the mitochondrial oxidase; the former compound reverses the glycerol kinase step that is most important during anaerobic glycolysis (6).

Computer modeling of glycolytic flux is feasible because kinetic quantities are known for all of the *T. brucei* glycolytic enzymes, and glycolysis in this protozoan exists as an isolated pathway. These studies successfully reproduced the observed metabolic flux without the need to adjust the experimentally determined kinetic parameters of the various steps, and thus yielded an analytical and nonbiased description of *T. brucei* glycolysis (7, 8). Such studies reveal that glucose import only partially controls overall glycolytic flux (verified experimentally), and the rate of the enzymatic steps catalyzed by GAPDH, phosphoglycerate kinase, and glycerol-3-phosphate dehydrogenase are also partly rate controlling (8). Computer modeling shows that competitive inhibitors of these three glycolytic enzymes significantly reduce glycolytic flux when ratios of $[I]/K_I$ are 10–100 (8), whereas inhibitors of other enzymes such as hexokinase have minimal effect (8, 9). Potent inhibitors that selectively block the parasite enzymes while leaving the human glycolytic enzymes unaffected are not yet available. Therefore, we decided to develop trypanosomatid-selective inhibitors of glycolytic enzymes by structure-based drug design.

Over the past several years we have determined the crystal structures of *T. brucei* and *L. mexicana* GAPDHs (10, 11), and the structure of the *T. cruzi* enzyme has been reported recently by Souza *et al.* (12). Comparison of these structures to the human GAPDH crystal structure (10, 13) reveals differences around the binding pocket for the adenosyl moiety of bound NAD^+ cosub-

The publication costs of this article were defrayed in part by page charge payment. This article must therefore be hereby marked "*advertisement*" in accordance with 18 U.S.C. §1734 solely to indicate this fact.

PNAS is available online at www.pnas.org.

This paper was submitted directly (Track II) to the *Proceedings* office.
Abbreviation: GAPDH, glyceraldehyde-3-phosphate dehydrogenase.
Data deposition: The structure has been deposited in the Protein Data Bank, Biology Department, Brookhaven National Laboratory, Upton, NY 11973 (PDB ID code 1gyq).
†Present address: Department of Pharmaceutical Chemistry, University of California, San Francisco, CA 94143-0446.
††To whom reprint requests should be addressed. e-mail: gelb@chem.washington.edu or hol@gouda.bmsc.washington.edu.

strate (14). This observation suggests that it may be possible to design compounds that selectively and competitively block the binding of NAD^+ to trypanosomatid GAPDHs. NAD^+ exhibits rather weak affinity for the parasite enzyme, with a K_M of 0.45 mM (15). Not surprisingly, adenosine is a very weak competitive inhibitor of *T. brucei* GAPDH with an IC_{50} of 50 mM (14). Despite widespread prejudice against the use of lead compounds with millimolar affinity for the macromolecular target, we nevertheless embarked on a structure-based design effort using adenosine as a lead (14). In this study, we describe the preparation of adenosine analogs with submicromolar affinity for trypanosomatid GAPDH. Such compounds are sufficiently potent to warrant examination of their effects on cultured parasites, and parasite growth and glycolytic flux measurements also are reported.

MATERIALS AND METHODS

Synthesis of Adenosine Analogs (see Scheme 1 below). Substituted 1-naphthalenemethylamines were prepared from corresponding naphthoic acids by using standard procedures (16). Compounds **2-8** were synthesized from 6-iodopurine riboside analogue **11** by using established methods (17) and were shown to be pure by reverse-phase HPLC analysis on a C_{18} column (Vydac 218TP1010) with a $MeOH/H_2O$ gradient.

*9-[2′-deoxy-2′-(3-methoxybenzamido)-3′,5′-O-(1,1,3,3-tetraisopropyldisiloxane-1,3-diyl]-(1-β-D-ribofuranosyl)-6-iodopurine (***10**). Starting material **9** (18) was iodinated essentially as described (19). To a stirred solution of **9** (25 mg, 51 μmol) in 10 ml of dry tetrahydrofuran, diiodomethane (50 μl, 0.63 mmol), iodine (16 mg, 0.063 mmol), and CuI (12 mg, 0.063 mmol) were added under Ar, and the mixture was heated to reflux. Isoamyl nitrite (25 μl, 0.19 mmol) was added slowly by syringe, and the mixture was refluxed until no starting material was observed by TLC. The solvent was removed *in vacuo*, and the solid residue was redissolved in $CHCl_3$ and loaded onto silica gel. Chloroform was applied until red coloration caused by iodine was no longer visible, and the product was eluted with 3:1 $CHCl_3$/ethyl acetate. Yield 19 mg (50%). ^1H NMR ($CDCl_3$) δ 0.95–1.3 (m, 28, 4 *i*Pr), 3.81 (s, 3, MeO), 4.08 (m, 3, H4′, 5′, 5′′), 4.86 (m, 1, H2′), 5.42 (t, 1, H3′), 6.10 (d, 1, H1′), 7.05–7.4 (m, 9, aromatic protons), 8.33 (s, 1, H2), 8.53 (s, 1, H8).

*9-[2′-deoxy-2′-(3-methoxybenzamido)]-(1-β-D-ribofuranosyl)-6-iodopurine (***11**). The deprotection procedure described for **1** (18) starting with 10 mg (13.2 μmol) of **10** produced 6 mg (89%) of the title product, which was purified on silica with an ethyl acetate/MeOH gradient. ^1H NMR δ 3.81 (s, 3, MeO), 3.85 (dd, 1, H5′), 3.92 (dd, 1, H5′′), 4.28 (m, 1, H4′), 4.53 (dd, 1, H3′), 5.33 (m, 1, H2′), 6.32 (d, 1, H1′), 7.1–7.4 (m, 4, aromatic protons), 8.22 (d, 1, NH), 8.55 (s, 1, H2), 8.82 (s, 1, H8).

*N-6-(1-napthalenemethyl)-2′-deoxy-2′-(3-methoxybenzamido)-adenosine (***5**). ^1H NMR (MeOH-d_4) δ 3.78 (s, 3, MeO), 3.80 (dd, 1, H5′), 3.95 (dd, 1, H5′′), 4.30 (m, 1, H4′), 4.52 (dd, 1, H3′), 5.20 (s, 2, CH_2), 5.41 (m, 1, H2′), 6.21 (d, 1, H1′), 7.0–7.6 (m, 8, benzamide + 4 naphthalene β-protons), 7.8–8.1 (m, 3, 3 naphthalene α-protons), 8.21 (s, 2, H2, 8).

N-6-benzyladenosine-5′-phosphate. N^6-benzyladenosine was phosphorylated by using conditions developed by Yoshikawa *et al.* (20). An aliquot was purified by HPLC for identification by NMR. The yield was estimated to be quantitative by NMR in D_2O with MeOH as internal standard. ^1H NMR (D_2O) δ 3.33 (s, 2, CH_2), 4.16 (m, 1, H5′), 4.22 (m, 1, H5′′), 4.27 (m, 1, H4′), 4.39 (t, 1, H3′), 4.62 (t, 1, H2′), 6.10 (d, 1, H1′), 7.28–7.40 (m, 5, aromatic protons), 8.31 (s, 1, H2), 8.48 (s, 1, H8).

N-6-benzyl-NAD$^+$. N^6-benzyladenosine-5′-phosphate was coupled to nicotinamide mononucleotide essentially as described (21). As part of the final work-up, the solvent was removed *in vacuo*, and the solid residue was redissolved in 10 ml of water. The pH was adjusted to 2 with 2 N HCl, and the NAD^+ analogue was purified by reverse-phase HPLC using a $MeOH/H_2O$ gradient containing 0.05% trifluoroacetic acid. Yield 20 mg (8.8%). ESI MS ($M\text{-}H^+$) 752.5.

Molecular Modeling. Initially, adenosine derivatives were docked visually in the *T. brucei* GAPDH structure with the BIOGRAF modeling package (22). Subsequently, the most promising inhibitors were docked by Monte Carlo methods with QXP software (23).

Crystallography. *L. mexicana* GAPDH was expressed in *Escherichia coli* as described (11). Cocrystals with N^6-benzyl-NAD^+ were grown in sitting drops: 2 μl of a solution containing 2.25 mg/ml of *L. mexicana* GAPDH, 1 mM DTT, 1 mM EDTA, 1 mM phenylmethylsulfonyl fluoride, and 0.4 mM N^6-benzyl-NAD^+ in 10 mM triethanolamine buffer, pH 7.0 was mixed with 1 μl of reservoir solution, containing 25% PEG 5000 monomethyl ether

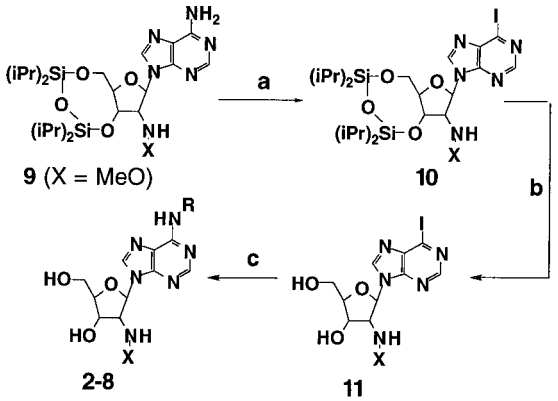

(a) CH_2Cl_2, I_2, CuI, THF; (b) NH_4F, MeOH; (c) RNH_2, Et_3N, MeOH

SCHEME 1.

and 100 mM Tris, pH 8.0. These drops were equilibrated against the reservoir. For cryoprotection the crystals first were transferred to an artificial mother liquor containing 26% PEG 5000 monomethyl ether, 100 mM triethanolamine (pH 7.6), 10 mM DTT, and 0.5 mM N^6-benzyl-NAD^+ and then to the same liquor containing additionally 15% glycerol. The crystals were frozen in a stream of nitrogen, and data to 3.4 Å were collected at the Stanford Synchrotron Radiation Laboratory beam line 7–1. The space group was $P2_12_12_1$ with cell parameters $a = 97.3, b = 125.8, c = 137.8$ Å, close to the crystals with NAD^+ (11). Rigid-body refinement of each of the four subunits of the tetramer resulted in an R factor of 30%, after which electron density could be observed for the bound N^6-benzyl-NAD^+ molecules. Four-fold noncrystallographic symmetry averaging (24) of only the protein resulted in considerable improvement of the map and unambiguous density for the modified cofactor in all four binding sites (Fig. 1). Because of the limited resolution, individual atomic positional refinement was not pursued.

Studies with Cultured Parasites. *T. cruzi* (Tulahuen strain from S. Reed, Corixa Corporation) was stably transfected with the *E. coli* β-galactosidase gene (*LacZ*). Mammalian stage parasites (trypomastigotes and amastigotes) were grown on monolayers of 3T3 fibroblasts in DMEM containing 10% FBS, penicillin, and streptomycin at 37°C with 5% CO_2. Parasite growth was determined at 7 days by measuring β-galactosidase activity (25). Bloodstream form *T. brucei brucei* (strain 427 from K. Stuart, Seattle Biomedical Research Institute) were cultured in HMI-9 medium containing 10% FCS, penicillin, and streptomycin at 37°C with 5% CO_2. The growth of *T. brucei* and murine NIH 3T3 fibroblasts was determined with Alamar Blue (Alamar Biosciences, Sacramento, CA) at 48 h and 5 days, respectively (26). Alamar Blue quantitation of *T. brucei* corresponded with visual counts determined with a hemacytometer.

Excretion of pyruvate from *T. brucei* bloodstream form into the media was measured by transferring cells from a midlog culture into balanced salt solution (50 mM NaCl/5 mM KCl/50 mM Bicine, pH 8.0) containing 0.1% BSA, 10 mM glucose (27), and various amounts of adenosine analog or DMSO vehicle (5×10^6 parasites/ml) at room temperature (20°C). At the indicated times, 750-μl aliquots were withdrawn. After pelleting parasites by centrifugation, the supernatants were frozen for up to 6 h before pyruvate analysis. Pyruvate was quantified by adding 50- to 200-μl sample to 0.5 ml of 100 mM Hepes, pH 8.0 containing 0.4 mM NADH, and the total volume was brought to 1 ml with balanced salt solution/BSA/glucose. Sufficient lactate dehydrogenase (Sigma) was added so that the drop in absorbance at 340 nm was complete in less than 15 min. Under these conditions, all of the pyruvate was converted to lactate, and the drop in OD_{340} was proportional to the moles of pyruvate present in the parasite supernatant. Each assay was routinely calibrated by adding standard pyruvate to the mixture after the first drop in OD_{340} was complete and recording the second drop.

RESULTS

Adenosine Derivatives as Trypanosomatid-Selective GAPDH Inhibitors. Attachment of 2′ aromatic substituents to adenosine significantly improves binding to trypanosomatid GAPDH while preventing binding to the human homolog (14). The 2′-(3-methoxybenzamido) group improves the binding of adenosine to *L. mexicana* GAPDH by 50-fold (compound **1**) (14). This substituent could be modeled into a narrow hydrophobic cleft, the selectivity cleft, that exists in trypanosomatid GAPDHs but is occluded in the human enzyme. The alteration in cleft size is caused by different local backbone conformations for these two enzymes. The selectivity cleft starts with a conserved Asp residue that accepts a hydrogen bond from the O2′ hydroxyl of adenosine and continues with hydrophobic walls formed by Met-39 on one side and Val-206* on the other side; the latter residue belongs to a neighboring subunit of the tetrameric enzyme. Use of a 2′ amido group rather than an ester is predicted to preserve the hydrogen bond (Asp-38-CO_2^-···HNCO). Additional structure-based design led to 8-thienyladenosine, which binds 100-fold tighter than adenosine to trypanosomatid GAPDH (14). However, combining 2′ and 8 substituents on the adenosine scaffold led to disappointing inhibition results probably because the carbonyl oxygen of the 2′ substituent is predicted to clash with the thienyl ring when the adenosine analog assumes its bound conformation in the active site of GAPDH (28).

The environment of GAPDH near N^6 of adenosine is quite hydrophobic as it is formed by the side chains of Met-39, Ala-90, Leu-113, and Phe-114 and the side chain methylene units of Arg-92. The N^6 amino group itself is a hydrogen bond donor to the backbone carbonyl of Gln-91. Screening of commercially available N^6-substituted adenosine derivatives afforded several hits with an 8- to 12-fold gain in affinity compared with adenosine (29). These hits all possess secondary amine functionalities, which could serve as hydrogen bond donors, and displayed IC_{50} values in the 3- to 5-mM range. One of the hits was N^6-benzyladenosine ($IC_{50} = 5$ mM).

Structure of the N^6-Benzyl-NAD^+·*L. mexicana* GAPDH Complex. Optimization of the N^6 substituent would be facilitated by determining the structure of an N^6-substituted adenosine bound to trypanosomatid GAPDH. Because *L. mexicana* GAPDH is expressed much better in *E. coli* than the *T. brucei* enzyme, crystallization studies were carried out with the former. These enzymes share 81% identity, and the adenosine binding sites of these two enzymes are virtually identical (however, see below), with 0.2-Å rms deviation on backbone and 0.5 Å on side-chain atom positions (10, 11). Also, the structure of *T. cruzi* GAPDH appears virtually identical in the targeted area of the active site (12). After several unsuccessful attempts to obtain N^6-benzyladenosine·*L. mexicana* GAPDH cocrystals (*L. mexicana* apo-GAPDH also resists crystallization), we turned to the synthesis of N^6-benzyl-NAD^+ because robust crystallization condi-

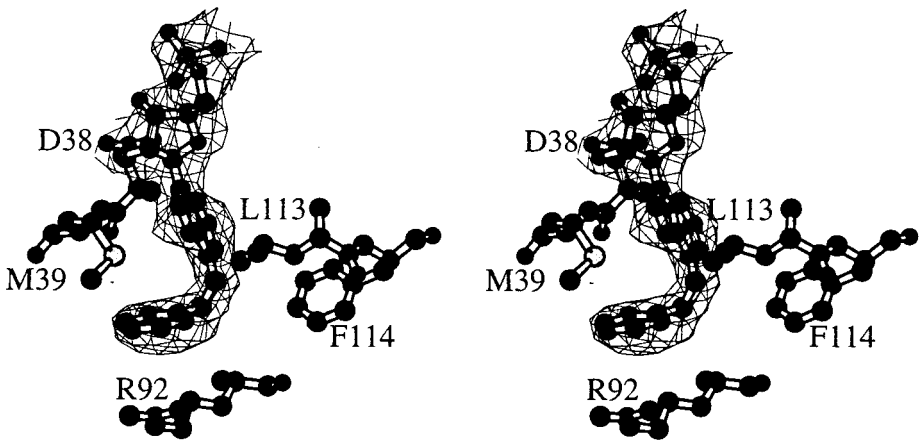

FIG. 1. Stereoview of the final electron density map for N^6-benzyl-NAD^+ bound to *L. mexicana* GAPDH.

tions already had been developed for the enzyme-NAD^+·complex (11). Not only was N^6-benzyl-NAD^+ a good substrate for *L. mexicana* GAPDH (K_M = 250 μM versus 450 μM for NAD^+; $V_{max}(NAD^+)/V_{max}(BnNAD^+)$= 6), but crystals of the enzyme-substrate analog complex suitable for x-ray analysis were obtained as described in *Materials and Methods*.

The derived x-ray structure of the complex shows that the benzyl group is sandwiched between the side chains of Met-39 and Arg-92 and also contacts Ala-90 (Fig. 1). The nonbenzyl atoms of N^6-benzyl-NAD^+ superimpose onto the corresponding atoms of NAD^+ in the original structure of *L. mexicana* GAPDH (11). In our previous study, we pointed out that the N^6-benzyl group could be modeled into two clefts (29). One of the clefts corresponds precisely to the observed binding site for the N^6-benzyl group of the NAD^+ analog. Occupancy of the other cleft would have required substantial repositioning of the benzyl group such that it would contact Leu-113 and Phe-114 (29). The structure in Fig. 1 suggests that smaller hydrocarbons would not fill the N^6-pocket as well as benzyl. This observation is consistent with our earlier studies in which we showed that N^6-isopropyl, *t*-butyl, 2-amyl, and cyclopentyl substituted adenosines bound at least 5-fold weaker than N^6-benzyladenosine to *L. mexicana* GAPDH (29). Groups larger than these small hydrocarbons, cycloheptyl, cyclopentyl, and 2-methylbutyl all bound with affinity comparable to that of N^6-benzyladenosine.

1-Naphthalenemethyl as a Preferred N^6-Adenosine Substituent. Of all the N^6-substituted adenosines studied previously, N^6-(1-naphthalenemethyl)adenosine was the most potent inhibitor of *L. mexicana* GAPDH with an IC_{50} of 150 μM, 33-fold more potent than N^6-benzyladenosine and 330-fold more potent than adenosine (29). To search for a structural explanation for improved binding with the naphthalene substituent, we modeled this bicyclic hydrocarbon into the same cleft that is occupied by the benzyl group. As shown in Fig. 2, an excellent fit on the surface of *L. mexicana* GAPDH was found. In this modeled orientation, all of the CH groups of naphthalene are in van der Waals contact with GAPDH except for C4 and C7. The naphthalene is sandwiched between the methylenes of the side chain of Arg-92 and the side chain of Met-39 as for the benzyl group. The planes occupied by the naphthalenemethyl and benzyl groups are nearly the same.

Because the N^6 and 2′ adenosine substituents point in entirely different directions, it should be possible to combine them onto the same adenosine scaffold to maximize inhibition. Thus, we prepared N^6-(1-naphthalenemethyl)-2′-(3-methoxybenzamido) adenosine (compound **5**). This compound inhibits *L. mexicana* GAPDH with an IC_{50} of 0.28 μM, which is more than five orders of magnitude lower than the IC_{50} of adenosine, our original lead compound (Table 1). In addition, **5** does not detectably inhibit human GAPDH when tested up to its solubility limit of approximately 40 μM. Fig. 3 shows the modeled structure of **5** in the active site of *L. mexicana* GAPDH. It suggests how the selectivity

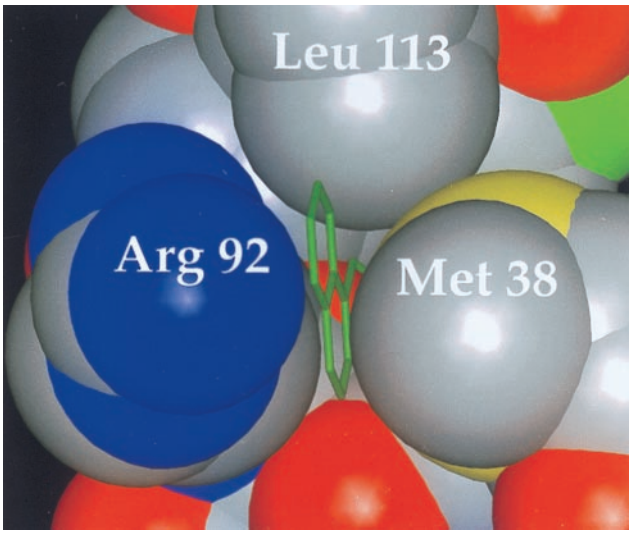

FIG. 2 Naphthalenemethyl moiety of N^6-1-naphthalenemethyladenosine modeled into the N^6-pocket of *L. mexicana* GAPDH. Atoms of GAPDH are shown with a doubled van der Waals surface.

cleft and the N^6 substituent pocket simultaneously are occupied by the disubstituted nucleoside **5**. A Lineweaver-Burke analysis of *L. mexicana* GAPDH inhibition by **5** shows the intersecting line pattern typical of competitive inhibition when [NAD^+] and **5** are varied (not shown).

We prepared a number of variants of **5** that contained substituents on the naphthalene ring. IC_{50} results are summarized in Table 1. Addition of a methyl group to C7 of naphthalene (**7**) led to a 18-fold increase in IC_{50}, and an aminomethyl group at C4 (**6**) abrogated inhibition. Furthermore, addition of all of the following substituents to the naphthalene ring of **5** led to inferior inhibitors (20- to 3,500-fold higher IC_{50} values; ref. 16): 2-methyl, 4-amino, 4-chloro, 4-methoxy, 6-methoxy, 6-hydroxy, 7-carboxy, and 8-aminomethyl. This structure-activity data is consistent with the model shown in Fig. 2. Visual inspection of the model suggests that all of the naphthalene substituents undergo significant van der Waals clash with GAPDH residues. The same can be said of compounds with modified N^6-benzyl groups (compounds **2**, **3**, and **4**), which are much less potent than **5** (Table 1).

Finally, we prepared the analog of **5** with the methoxy group on the 2′ substituent replaced with chlorine. Compound **8** was 36-fold less potent than **5** against *L. mexicana* GAPDH. This result was surprising given the fact that 2′-(3-chlorobenzamido)adenosine displays an IC_{50} of 90 μM, which is 9-fold smaller than the value for the 3-methoxy compound (16).

All of the naphthalene-containing adenosine compounds shown in Table 1 (except **8**) are 8- to 12-fold more potent on *L. mexicana* GAPDH than on the *T. brucei* and *T. cruzi* enzymes;

Table 1. Effect of adenosine analogues on trypansomatid GAPDH (IC_{50}) and on growth of cultured parasites (ED_{50})

Compound	*L. mexicana*, IC_{50}	*T. brucei*, IC_{50}†	*T. brucei*, ED_{50}‡	*T. cruzi*, IC_{50}	*T. cruzi*, ED_{50}	3T3 fibroblasts,* ED_{50}
Adenosine	5×10^4	10^5	>50	10^5	>50	>50
2	>100		>50		20	>50
3	150		>50		>50	>50
4	80		>50		>50	>50
5	0.28	2	30	5	12	>50
6	83	>1,000	>50	>1,000	>50	>50
7	5	25	50	45	20	>50
8	10	30	15	14	3	45

All values are in μM.
*Noninfected host cells used to support growth of *T. cruzi* amastigotes.
†IC_{50} values were determined by measuring GAPDH inhibition at 3–5 concentrations (10% error) (29).
‡Statistical error limits on the ED_{50} values determined in triplicate are 15% (20% for separate experiments).

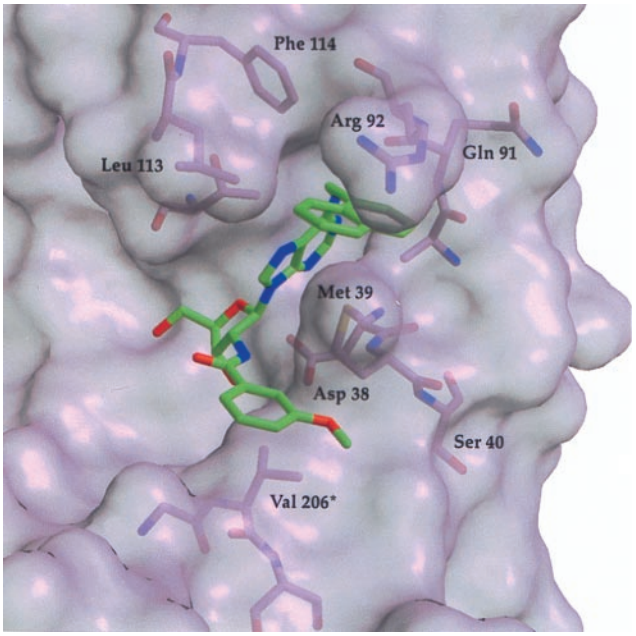

FIG. 3. RASTER3D (30) model showing inhibitor **5** docked into the adenosine binding pocket of *L. mexicana* GAPDH. The H-bonds between N^6-H of **5** and C=O of Gln-91 and 2′-NH of **5** and CO_2^- of Asp-38 are not drawn.

IC_{50}s of the compounds for the latter two enzymes are virtually identical (Table 1). Considering the GAPDH residues that are predicted to contact bound **5**, the only difference in these structures occurs in the selectivity cleft. *L. mexicana* GAPDH has a serine near position 3 of the 2′-benzamido substituent (Ser-40), whereas the *T. brucei* and *T. cruzi* enzymes have an asparagine at this position. It is not obvious why the serine-to-asparagine change causes a reduction in the affinity of 2′,N^6-disubstituted adenosines. Such small changes in affinity (only 1.4 kcal/mol in energy terms) are often difficult to interpret.

Trypanosomatid Growth Inhibition Studies. A subset of the compounds prepared in this study were tested for their ability to block the growth of bloodstream *T. brucei*. For these studies we chose to work with *T. brucei brucei* strain 427, which is adapted to grow in culture as its bloodstream form stage (31). Previous studies have shown that this strain derives virtually all of its energy from the glycolytic conversion of glucose to pyruvate (31). As shown in Fig. 4, compound **8** is toxic to bloodstream *T. brucei* with an ED_{50} of 15 μM. Our most potent inhibitor **5** was 2-fold less effective than **8** against *T. brucei*. A further 2-fold drop in activity was observed for the 7-methylnaphthyl analogue **7**. Adenosine was not toxic to parasites up to 50 mM, the highest concentration tested.

We also tested these adenosine analogs for their ability to inhibit the growth of the intracellular form (amastigotes) of *T. cruzi* present in 3T3 fibroblast host cells. As described in *Materials and Methods*, we used a genetically engineered strain of *T. cruzi* so that parasite growth could be readily monitored with a colorimetric assay. Our glycolytic inhibitors were effective at killing *T. cruzi* amastigotes, with relative potencies of adenosine analogues generally similar to the values obtained with *T. brucei* (Fig. 4). Compound **8** was again the most potent analogue, with an ED_{50} of 3 μM. None of the compounds tested had any effect on the growth of 3T3 fibroblasts in the control experiment, except for **8**, which inhibited 50% of the growth when tested at 50 μM, but was nontoxic up to 30 μM (not shown). Fig. 5 shows optical microscope pictures of infected host cells treated with varying doses of **8**.

GAPDH Inhibitors Block *T. brucei* Glycolysis. Glycolytic flux in bloodstream *T. brucei* can be readily monitored by transferring cells from a midlog phase culture to balanced salt solution containing glucose and monitoring pyruvate production in the extracellular fluid. Based on the stoichiometry of glycolysis, the rate of pyruvate secretion into the medium equals twice the glycolytic flux. As shown in Fig. 4, when parasites are transferred to balanced salt solution containing **8**, pyruvate accumulation slows after 20 min in a dose-dependent manner. Additionally, visualization of parasites by optical microscopy clearly showed that motility ceases within minutes after addition of **8**, whereas parasites continued to be motile for at least 12 h in glucose-supplemented balanced salt solution in the absence of GAPDH inhibitor. Accompanying the loss of motility, parasite shape changed from the typical elongated flagellated morphology of the bloodstream form to rounded forms, and parasite lysis was also apparent (not shown). Concentrations up to 40 μM of the poor GAPDH inhibitor **6** had no effect on pyruvate production, motility, and cell shape (not shown).

DISCUSSION

The results of the present study underscore the usefulness of a structure-based approach to dramatically improve the target affinity of a mediocre lead compound, adenosine in this case. They also show that limited structural differences between the human and trypanosomatid GAPDHs can be exploited to obtain inhibitors that are >50-fold selective. No additional improvement in selectivity is needed because **5** does not inhibit human GAPDH when present at its solubility limit. Human GAPDH, like the trypanosomatid enzyme, has a region that can accommodate a hydrophobic N^6 adenosine substituent. In fact, the corresponding sites on these enzymes are identical except that human GAPDH has valine in place of leucine at position 113. The fact that engagement of the N^6-(1-naphthalenemethyl) group with the hydrophobic slot on GAPDH probably requires simultaneous positioning of the 2′-(3-methoxybenzamido) group into the se-

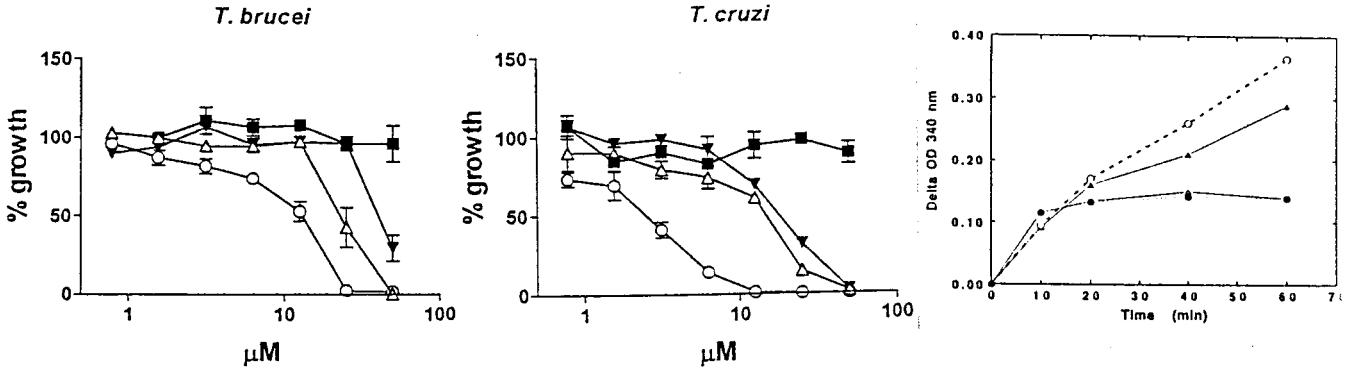

FIG. 4. Growth inhibition of *T. brucei* bloodstream form (*Left*) and *T. cruzi* amastigotes in 3T3 host cells (*Middle*) in the presence of adenosine (■) and GAPDH inhibitors **5** (△), **7** (▼), and **8** (○). Pyruvate production in bloodstream *T. brucei* after addition of 0 (○), 12 (▲), 24 (△), and 40 μM (●) **8** (*Right*) (△ and ● overlap in parts).

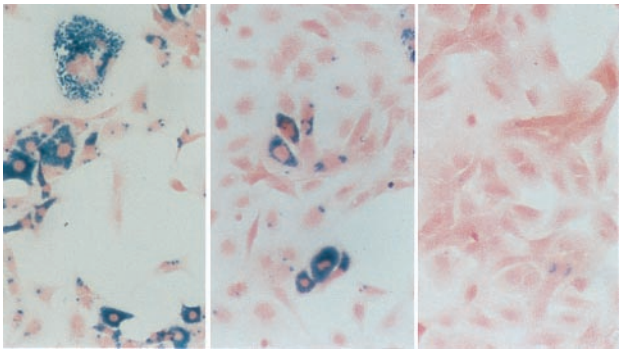

FIG. 5. Optical microscopy showing 3T3 fibroblasts infected with *T. cruzi* amastigotes on addition of 0 (*Left*), 16 (*Middle*), and 40 μM (*Right*) **8**. After fixation, cells were stained with 5-bromo-4-chloro-3-indolyl β-D-galactoside to assay β-galactosidase and counter-stained with Safranin O.

lectivity cleft would prevent the disubstituted adenosine analog from binding to the human enzyme. One inherent difficulty with structure-based drug design stems from our inability to accurately calculate binding energies of protein-ligand complexes. Not surprisingly, the binding energetics for the N^6 and 2′ substituents interacting with their respective sites on GAPDH are coupled. This coupling is apparent from the fact that although the chlorine at position 3 of the 2′-benzamido group promotes GAPDH binding more than a methoxy group when attached to adenosine, methoxy is the better substituent when the adenosine analog also bears the N^6-(1-naphthalenemethyl) group (Table 1). This result suggests that a combinatorial chemical approach that focuses on the 2′ and N^6 positions is a logical next step for obtaining inhibitors of GAPDH that are more potent than **5**. The value of the x-ray structure analysis in guiding us to the 2′ and N^6 positions for substituent attachment should not be underestimated. Adenosine contains 11 atoms that can bear substituents, and when one also considers stereochemistry, there are 120 unique two-substituent combinations.

Reluctance of using adenosine as an inhibitor scaffold stems from the fact that many human enzymes exist that bind adenosyl-containing cofactors and cosubstrates. However, the three-dimensional shape of a molecule like **5** is a significant departure from that of an unsubstituted nucleoside. These adenosine analogs may be structurally as different from adenosine as an HIV protease inhibitor is distant from poly-alanine. Compound **5** was shown to be completely inactive against a number of ATP- and NAD^+-dependent enzymes, such as phosphoglycerate kinase, lactate dehydrogenase, and glycerol-3-phosphate dehydrogenase. Another positive feature of these nucleoside analogs is that they are considerably more hydrophobic than adenosine and might be expected to pass through the trypanosomatid membrane by passive diffusion. This feature would circumvent the potential problem of drug resistance caused by mutations in a nucleoside transporter. The mode of uptake of compounds such as **5** by parasites remains to be established. Compound **5** has a molecular weight of 540, which is in the range acceptable for small molecule drugs.

The fact that our most potent GAPDH inhibitors are capable of killing bloodstream *T. brucei* and *T. cruzi* amastigotes is consistent with the idea that at least some of the glycolytic enzymes are good targets for drug design. Our results are also consistent with the computational studies of Bakker and Westerhoff (7, 8), who showed that GAPDH is one of the enzymes that partially controls the overall flux of glycolysis in bloodstream *T. brucei*. These investigators measured the flux control coefficient for glucose import into parasites and found that this step only partially controls metabolic flux, which proves that one or more additional steps in the pathway also exert control. Although compound **8** was found to block glycolytic flux (cessation of pyruvate production), we cannot rule out the possibility that this compound kills parasites for reasons other than shutdown of glycolysis. The problem is that survival of bloodstream *T. brucei* and glycolysis are tightly coupled, making it difficult to tease these two events apart. It may be possible to design mutations in *T. brucei* GAPDH that abrogates binding to 2′, N^6-disubstituted adenosine analogs and to determine whether expression of such a protein *in vivo* allows the parasite to survive inhibitor treatment. The fact that addition of small substituents, including a methyl group to the naphthalene ring of our adenosine analogs, reduces GAPDH affinity, potency for killing parasites and pyruvate production is consistent with glycolysis as the target for these agents. The relatively small differences in the values of IC_{50} and ED_{50} could be suggestive of selective uptake that leads to elevated levels of the compounds inside the parasites: studies of parasite uptake of radiolabeled drugs could potentially resolve this issue.

1. W.H.O. (1991) *Control of Chagas' Disease* (W.H.O., Geneva), W.H.O. Technical Series #811.
2. Smith, D. H., Pepin, J. & Stich, A. H. R. (1998) *Brit. Med. Bull.* **54,** 341–355.
3. Pepin, J. & Milord, F. (1994) *Adv. Parasitol.* **33,** 1–47.
4. Clayton, C. E. & Michels, P. (1996) *Parasitol. Today* **12,** 465–471.
5. Engel, J. C., Franke de Cazzulo, B. M., Stoppani, A. O. M., Cannata, J. J. B. & Cazzulo, J. J. (1987) *Mol. Biochem. Parasitol.* **26,** 1–10.
6. Clarkson, A. B. & Brohn, F. H. (1976) *Science* **194,** 204–206.
7. Bakker, B. M., Michels, P. A. M., Opperdoes, F. R. & Westerhoff, H. V. (1997) *J. Biol. Chem.* **272,** 3207–3215.
8. Bakker, B. M. (1998) Ph.D Thesis (Free University of Amsterdam, The Netherlands).
9. Eisenthal, R. & Cornish-Bowden, A. (1998) *J. Biol. Chem.* **273,** 5500–5505.
10. Vellieux, F. M. D., Hajdu, J. & Hol, W. G. J. (1995) *Acta Crystallogr. D* **51,** 575–589.
11. Kim, H., Feil, I., Verlinde, C. L. M., Petra, P. H. & Hol, W. G. J. (1995) *Biochemistry* **34,** 14975–14986.
12. Souza, D. H. F., Garratt, R. C., Araujo, A. P. U., Guimaraes, B. G., Jesus, W. D. P., Michels, P. A. M., Hannaert, V. & Oliva, G. (1998) *FEBS Lett.* **424,** 131–135.
13. Mercer, W. D., Winn, S. I. & Watson, H. C. (1976) *J. Mol. Biol.* **104,** 277–283.
14. Verlinde, C. L., Callens, M., Van Calenbergh, S., Van Aerschot, A., Herdewijn, P., Hannaert, V., Michels, P. A., Opperdoes, F. R. & Hol, W. G. (1994) *J. Med. Chem.* **37,** 3605–3613.
15. Lambeir, A.-M., Loiseau, A. M., Kuntz, D. A., Vellieux, F. M., Michels, P. A. M. & Opperdoes, F. R. (1991) *Eur. J. Biochem.* **198,** 429–435.
16. Aronov, A. M. (1998) Ph.D. Thesis (University of Washington, Seattle).
17. Fleysher, M. H. (1972) *J. Med. Chem.* **15,** 187–191.
18. Van Calenbergh, S., Van Den Eeckhout, E., Herdewijn, P., De Bruyn, A., Verlinde, C., Hol, W. G. J., Callens, M., Van Aerschot, A. & Rozenski, J. (1994) *Helv. Chim. Acta* **77,** 631–644.
19. Matsuda, A., Shinozaki, M., Yamaguchi, T., Homma, H., Nomoto, R., Miyasaka, T., Watanabe, Y. & Abiru, T. (1992) *J. Med. Chem.* **35,** 241–252.
20. Yoshikawa, M., Kato, T. & Takenishi, T. (1967) *Tetrahedron Lett.* **11,** 5065.
21. Hughes, N. A., Kenner, G. W. & Todd, A. (1957) *J. Chem. Soc.,* 3733.
22. Molecular Simulations (1993) BIOGRAF 3.10 (Molecular Simulations, San Diego).
23. McMartin, C. & Bohacek, R. S. (1997) *J. Comput. Aided Mol. Des.* **11,** 333–344.
24. Kleywegt, G. J. & Jones, T. A. (1994) *From First Map to Final Model*, eds. Bailey, S., Hubbard, R. & Waller, D. (SERC Daresbury Laboratory, Warrington, U.K.), pp. 59–66.
25. Buckner, F. S., Verlinde, C. L. M. J., La Flamme, A. C. & Van Voorhis, W. C. (1996) *Antimicrob. Agents Chemother.* **40,** 2592–2597.
26. Ahmed, S. A., Gogal, R. M., Jr. & Walsh, J. E. (1994) *J. Immunol. Methods* **170,** 211–224.
27. Barnard, J. P., Reynafarje, B. & Pedersen, P. L. (1993) *J. Biol. Chem.* **268,** 3654–3661.
28. Van Calenbergh, S., Verlinde, C. L. M. J., Soenens, J., De Bruyn, A., Callens, M., Blaton, N. M., Peeters, O. M., Rozenski, J., Hol, W. G. J. & Herdewijn, P. (1995) *J. Med. Chem.* **38,** 3838–3849.
29. Aronov, A. M., Verlinde, C. L. M. J., Hol, W. G. J. & Gelb, M. H. (1998) *J. Med. Chem.* **41,** 4790–4799.
30. Merritt, E. A. & Bacon, D. J. (1997) *Macromol. Crystallogr. B* **277,** 505–524.
31. Cross, G. A. M. & Manning, J. C. (1973) *Parasitology* **67,** 315–331.